NASA Contractor Report 187119

Design, Optimization, and Analysis of a Self-Deploying PV Tent Array

Anthony J. Colozza
Sverdrup Technology, Inc.
Lewis Research Center Group
Brook Park, Ohio

June 1991

Prepared for
Lewis Research Center
Under Contract NAS3-25266

National Aeronautics and
Space Administration

DESIGN, OPTIMIZATION, AND ANALYSIS OF A SELF-DEPLOYING PV TENT ARRAY

Anthony J. Colozza
Sverdrup Technology, Inc.
Lewis Research Center Group
Brook Park, Ohio 44142

ABSTRACT

This study was performed in order to design a tent shaped PV array and optimize the design for maximum specific power. In order to minimize output power variation a tent angle of 60° was chosen. Based on the chosen tent angle an array structure was designed. The design considerations were minimal deployment time, high reliability and small stowage volume. To meet these considerations the array was chosen to be self-deployable, form a compact storage configuration, using a passive pressurized gas deployment mechanism. The array structural components consist of a combination of beams, columns and cables which are used to deploy and orient a flexible PV blanket to its proper configuration. Upon deployment pressurized gas is channeled to the columns causing them to extend, this deploys the PV blanket from the stowed configuration. Once extended the columns lock into place securing the structure. The arrangement and connection of the columns and the use of a thin flexible PV blanket was selected so that the array can be packaged into a relatively small volume.

Each structural component of the design was analyzed to determine the size necessary to withstand the various forces it would be subjected to. Through this analysis the component weights were determined. An optimization was performed to determine the array dimensions and blanket geometry which produce the maximum specific power for a given PV blanket. This optimization was performed for both Lunar and Martian environmental conditions. Other factors such as PV blanket type, structural material and wind velocity (for Mars array), were varied to determine what influence they had on the design point. The analysis showed that the variation of these parameters did not significantly affect the design points. These factors did, however, influence the array performance values, such as specific power and specific mass, at the design point. The performance specifications for the array at both locations and with each type of PV blanket were determined. These specifications were calculated using Arimid fiber composite as the structural material. This material produced the lowest specific mass out of the ones which were examined. The four PV blanket types considered were Silicon, GaAs/Ge, GaAs CLEFT and Amorphous Silicon. The specifications used for each blanket represented either present day or near term technology. For both the Moon and Mars the Amorphous Silicon arrays produced the highest specific power.

INTRODUCTION

The ability to establish an outpost or base in an isolated, harsh environment is initially dependent on the availability of an adequate power source. The ideal power supply would require very little implementation time and have a high reliability for operation. For space based applications it would also need to be lightweight and capable of being stowed in a relatively small volume. A device, such as a photovoltaic array, that is capable of meeting these requirements, would enhance mission versatility and thereby increase the ability to explore and establish bases on both the Moon and Mars or at remote Earth locations.

This study was therefore prompted by the realization of the unique exploration abilities which would be possible by having such a device. It was performed in order to design and optimize a tent-shaped array for both Lunar and Mars applications. A tent shape was chosen because, for a passive power collection device, it can produce a nearly constant power profile throughout the day time period, if the proper tent angle is selected (ref. 1). The array was designed to be self-deploying and use a flexible PV blanket for power generation. Pressurized gas expansion was chosen as the deployment mechanism because it reduces complexity over a mechanical system.

The array's tent configuration was analyzed with various PV blankets to determine the optimum PV blanket shape and array dimensions. The optimization was set up to determine design points which produced maximum specific power. The array design was based on the ability to meet the general requirements stated previously and to withstand the environmental conditions at the proposed location, either the Moon or Mars, where it would be used. The environment to which the arrays are designed can substantially influence their performance and configuration, therefore an array optimized for the Lunar surface would be different from one optimized for the Martian surface.

STRUCTURAL DESIGN

The structural design for the array uses a combination of cables, beams and columns to support and deploy the PV blanket. The cables used to support the PV blanket are attached to I-beams. The beams are held in their proper orientation by the columns, which also act as the deployment mechanism for the array. The columns consist of a series of hollow telescoping cylinders. Once extended these cylinders lock into place.

Deployment of the array is accomplished by the use of compressed gas released into the columns from a storage tank located at the base of the array. As the gas pressure in the columns increases they extend, deploying the PV blanket. The array is stowed with the blanket either folded or rolled, depending on the particular blanket's flexibility. The roll-out storage technique is preferable because it allows for easier repackaging if the array needs to be returned to its stowed configuration. Further details on the deployment mechanism and sequence are presented in appendix A.

An artist's conception of the deployment sequence for the tent array is shown in figure 1. The top and sides of the stowed array box have been omitted from this figure so the internal structure is visible.

ANALYSIS

The array structure had to be capable of supporting and orienting the PV blanket along with the ability for autonomous deployment and compact stowage. The analysis was performed by taking into account the various loadings on the structure and determining the optimum structural component size necessary to withstand them. The structural loadings are dependent on the blanket and array geometry, which is shown in figure B1 of appendix B.

The tent angle of the array, (that is, the angle a straight blanket would make with the horizontal), must be established before the analysis could begin. To determine a tent angle, one must consider the effect that this angle has on the output power profile. Figure 2 shows power profiles for various tent angles normalized to that of a tracking array. In order to minimize the mass of the power management and distribution system and any power storage device which may be used in conjunction with the array, a flat power profile is desired. This type of profile is needed because these other systems can be optimized to operate at only one power level. To maximize any power storage and management device

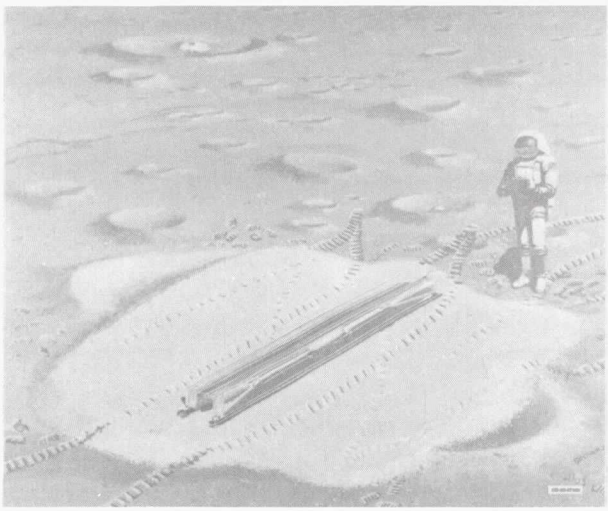

(a) Stowed configuration.

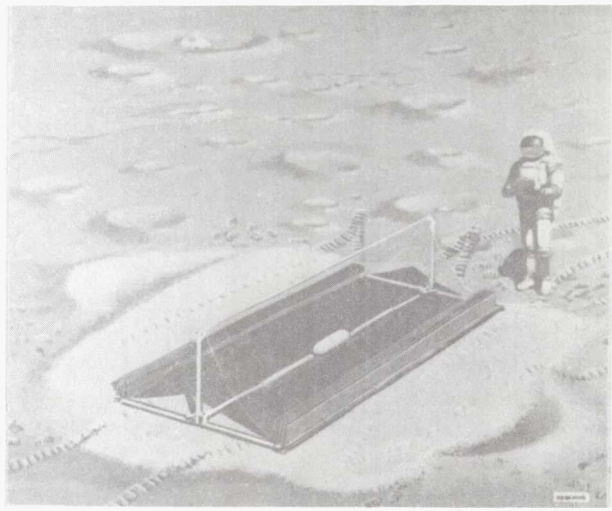

(b) Semi-deployed configuration.

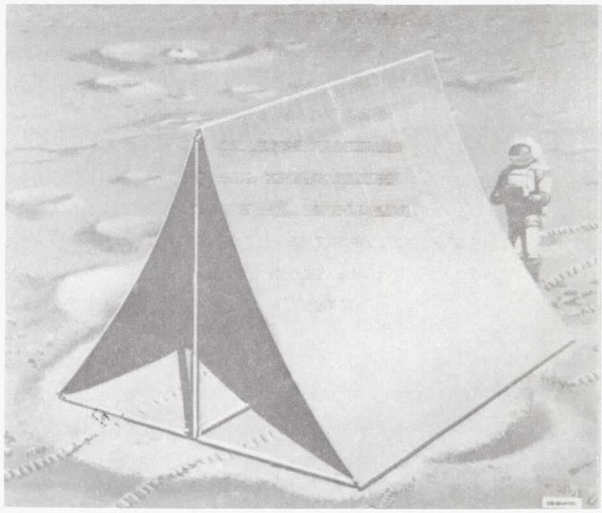

(c) Deployed configuration.

Figure 1.—Artist's drawing of deployment sequence for PV tent array.

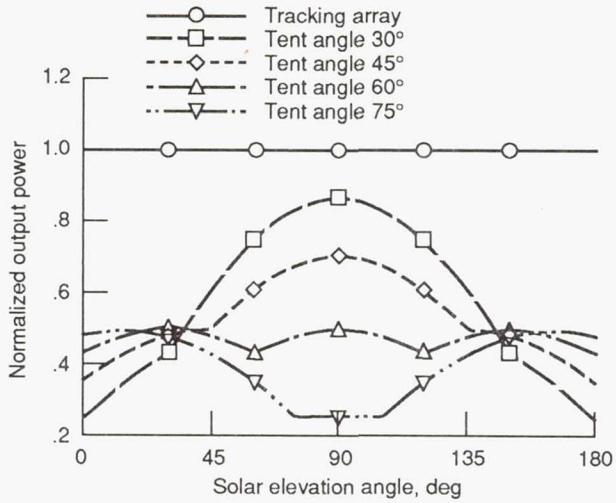

Figure 2.—Power profiles for arrays with various tent angles (output power is normalized to a tracking array value of 1).

TABLE I. - STRUCTURAL MATERIAL PROPERTIES

	Carbon VHS composite	Arimid fiber composite	Aluminum	Magnesium
Modulus, GPa	124	76	72	45
Yield strength, GPa	1.9	1.38	0.41	0.28
Density, kg/m^3	1530	1380	2800	1800

TABLE II. - PV BLANKET SPECIFICATIONS

	Silicon	GaAs/Ge	GaAs CLEFT	Amorphous silicon
Efficiency, percent	14.5	19.5	20.0	10.0
Cell thickness, μm	250	~250	20	2
Blanket specific Mass, kg/m^2	0.427	0.640	0.361	0.022
Technology status	Present Space Station technology	Present	Near-term	Future

efficiency, the input power to these systems should be kept as close to the systems design level as possible. A tent angle of 60° will minimize the output power variation throughout a day, so this angle was chosen as the array tent angle for the analysis (ref. 1).

A detailed description of the structural analysis used to determine the component weights and dimensions for different array geometries is given in appendix B. The geometry variables used are array width and PV blanket end angle. These variables were altered over a range of PV blanket areas until a combination was found which maximizes the array's specific power. This optimization was performed with various types of structural materials and for four types of PV blankets in both the Lunar and Martian environments. A list of the structural materials which were considered and their properties (ref. 2) are given in table I. The four PV blankets which were considered are silicon, gallium arsenide/germanium, CLEFT gallium arsenide and amorphous silicon. These blankets represent either present day or near-term technology. The specifications for these blankets (refs. 3 and 4) are listed in table 2.

The loads the structures must be capable of withstanding include wind loadings (Mars), the tension in the cables necessary to maintain a given blanket shape, and the force of gravity on the structure itself. On Earth, wind loadings are the dominant structural force. On Mars, however, the wind loadings are not nearly as great, due to the substantially lower atmospheric density. The Martian atmosphere at the planet surface has a density of 0.016 kg/m^3, similar to that at 30.5 km on Earth (ref. 5). On the Moon, where there is essentially no atmosphere, wind loadings are obviously not a problem. The cable tension, which is due to a combination of the desired blanket shape and the gravitational force, can be the driving force if wind loadings are not too severe. For the locations considered the gravitational acceleration is as follows (ref. 5): for Earth 9.81 m/s^2, for Mars 3.75 m/s^2, and for the Moon 1.61 m/s^2.

The PV blanket shape is determined by an optimization between reduction in tension and an increase in blanket area. Once the blanket shape is established, the optimum array dimensions can be found. The PV blanket shape and array dimensions characterize the array and set the optimum configuration for that array under the given environmental conditions.

Each component of the array was sized to withstand the forces it would be exposed to. The structural component masses were summed along with a fixed nonsizeable component mass to obtain the overall array structure mass. The nonsizeable component mass, estimated to be 4 kg, was used to account for such items as pressure lines, valves, column locking pins, pressurized seals and connection brackets for the columns and stowage box top and sides.

RESULTS

The first step in the optimization process was to determine the blanket shape, which is described by the blanket end angle. The end angle refers to the angle the PV blanket makes with the horizontal at the point where the blanket attaches to the array (angle θ_1 in fig. B1). Once this angle is chosen the blanket curvature, which is based on a catenary curve, and therefore cable tension is known for a particular size array. The array proportions (height to base) are fixed by selecting the tent angle, θ_t, which was taken to be 60° as discussed previously. The PV blanket area, and therefore array size, was varied for different end angle values. The results for a Mars based array with Arimid composite material, GaAs/Ge PV blanket, 20 m/sec wind velocity and a width of 5 m is shown in figure 3. On each curve of this figure there is an

array blanket area which corresponds to a minimum structural specific mass value. As the end angle decreases these minimum points shift toward larger array areas and lower specific masses.

The value of 5 m for the blanket width was found, by iterations with various array sizes and end angles, to be the optimum for the Mars based array. On the lunar surface, due to the different environment, lower gravity and lack of wind, the array width optimized at 6 m. Figure 4 shows array specific mass variation over a range of array widths for a Mars based array. This curve corresponds to the minimum specific mass point of the 0° end angle curve in figure 3. Both figures 3 and 4 are the final result of a long iterative process to determine the array geometric dimensions and blanket configuration which minimizes the array specific mass. It should be mentioned, however, that optimization at 0° end angle is not a universal truth. A combination of factors such as a weaker structural material, a heavier array blanket and more demanding environmental conditions could result in a non-0° end angle optimization.

The array dimensions and blanket geometry, obtained from figures 3 and 4, which give the minimum specific mass for the array are designated as the design points for the array. A similar procedure was followed to determine the design point for the Lunar based array.

The graphs presented so far are based on arrays which use Arimid fibers as the structural material, a GaAs/Ge cell PV blanket and, for the Mars-based array, a wind velocity of 20 m/sec. It was then necessary to determine what effect varying these parameters has on the design points which were generated for each array.

To determine the effect different structural materials have on the design point, array specific mass was calculated for four different structural materials over a range of array sizes. A graph of this data for the Mars tent array is shown in figure 5. These curves are based on a 60° Mars tent array with 0° end angle and a width of 5 m. By examining these curves it should be noted that the minimum points vary somewhat with different materials. Therefore the design points are dependent on the type of structural material used. Throughout this study Arimid fiber composite was used as the structural material. Of the materials given in figure 5 it produces the lowest specific mass.

The PV blanket has two parameters which can directly influence the analysis results. These are its specific mass and its energy conversion efficiency. The specific mass of the blanket directly affects the tension in the blanket support cables, which therefore influences the rest of the structural sizing. To determine the effect of a change in blanket weight on the design points, array specific mass for various types of PV blankets was calculated over a range of array sizes, as shown in figure 6. By examining the curves it can be seen that the minimum specific mass point, design point, is not dependent on blanket type. The energy conversion efficiency is used only to determine an absolute value for the specific power of the array. Therefore it will not influence the design characteristics and is not a factor in determining the design point for the array.

The last factor examined was wind loading. This factor, of course, only pertains to the Mars based array. Array specific mass for a number of wind loadings over a range of array sizes is shown in figure 7. It was determined that variations in wind loading did not effect the optimization or design point. It does, however, alter the actual value of array specific mass, and therefore array specific power for a given PV blanket.

Once the design points were established, calculations were made to determine the performance specifications of the array with each type of PV blanket. The design points, for both Lunar and

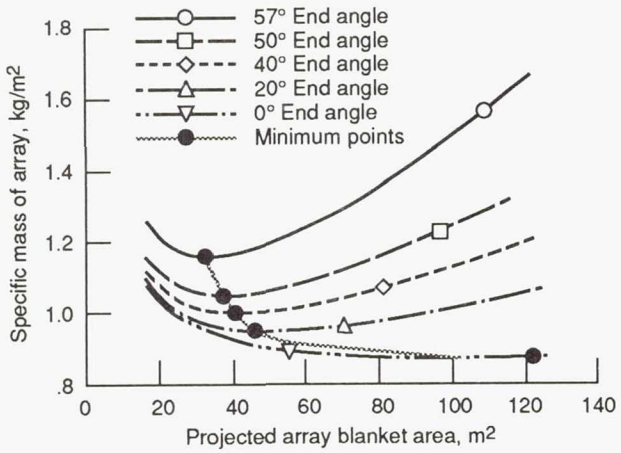

Figure 3.—Specific mass for various PV blanket lower end angles (60° Mars tent array with Arimid composite material, GaAs/Ge blanket and 20 m/s wind velocity).

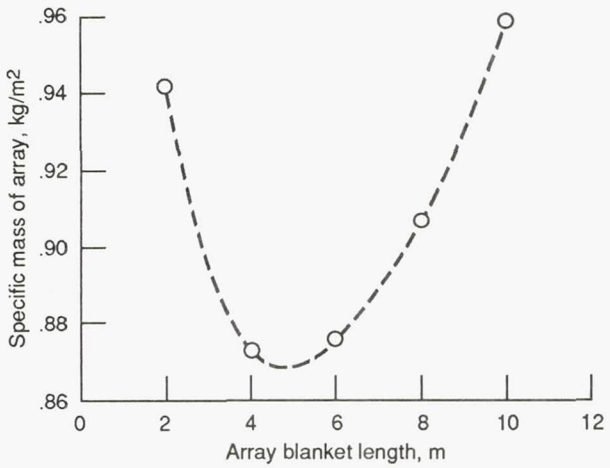

Figure 4.—Specific mass variation with array width (60° Mars tent array with Arimid composite material, GaAs/Ge blanket and 20 m/s wind velocity).

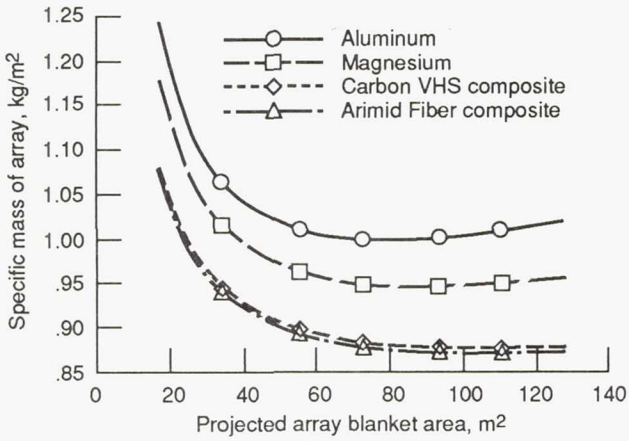

Figure 5.—Array specific mass for various structural materials (60° Mars tent array with GaAs/Ge blanket, 0° end angle, 20 m/s wind velocity, and 5 m width).

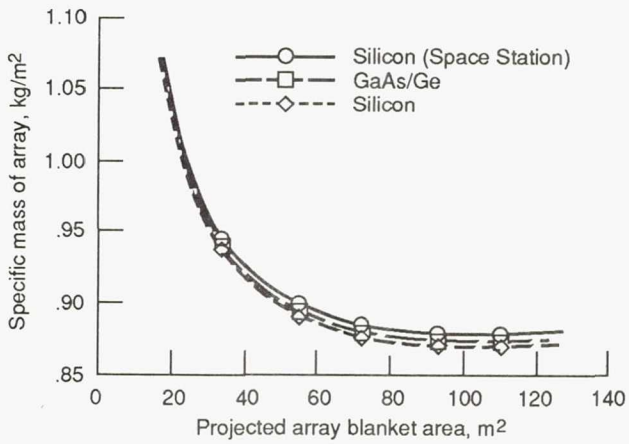

Figure 6.—Specific mass for various PV blanket types (60° Mars tent array with 0° end angle, Arimid composite material, 20 m/s wind velocity, and 5 m width).

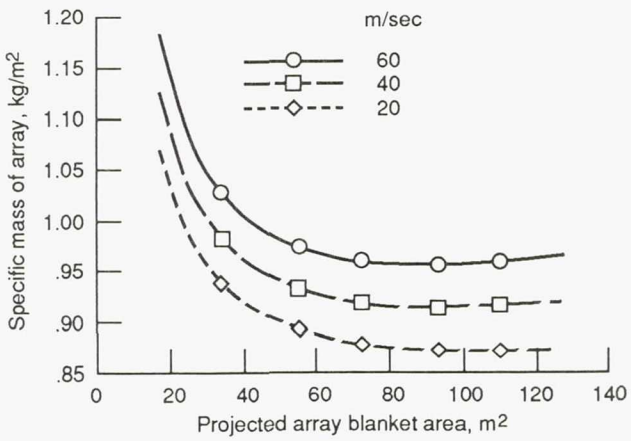

Figure 7.—Specific mass for various wind velocities (60° Mars tent array with 0° end angle, Arimid composite material, GaAs/Ge blanket, and 5 m width).

TABLE III. - GEOMETRY CHARACTERISTICS FOR ARRAY DESIGN POINTS

	Lunar based	Mars based
Tent angle, deg	60	60
End angle, deg	0	0
Array width, m	6.00	5.00
Array height, m	10.39	10.39
Array base, m	12.00	12.00
Blanket length, m	12.74	12.47
Blanket area, m^2	152.88	127.40

TABLE IV. - PERFORMANCE RESULTS FOR LUNAR TENT ARRAY

	Silicon	GaAs/Ge	GaAs CLEFT	Amorphous silicon
Structure mass, kg	26.27	27.30	25.92	22.86
Blanket mass, kg	65.25	97.86	55.19	3.36
Total mass, kg	91.53	125.16	81.11	26.22
Structure specific mass, kg/m^2	0.17	0.18	0.17	0.15
Array total specific mass, kg/m^2	0.60	0.82	0.53	0.17
Average output power, kW	13.36	17.96	18.41	9.21
Array specific power, W/kg	145.90	143.49	227.07	351.20

TABLE V. - PERFORMANCE RESULTS FOR LUNAR TENT ARRAY

	Silicon	GaAs/Ge	GaAs CLEFT	Amorphous silicon
Structure mass, kg	28.69	29.22	28.53	27.59
Blanket mass, kg	54.37	81.55	40.26	2.80
Total mass, kg	83.07	110.77	68.79	30.40
Structure specific mass, kg/m^2	0.23	0.23	0.22	0.22
Array total specific mass, kg/m^2	0.65	0.87	0.54	0.24
Average output power, kW	4.07	5.47	5.61	2.80
Array specific power, W/kg	48.95	49.36	81.52	92.24

Mars arrays, are given in table III. The performance specifications for all array/ PV blanket type combinations are given in tables IV and V.

CONCLUSION

The analysis performed on the array structure and PV blankets to determine the performance of the arrays were based on various assumptions and or approximations. Therefore the actual values obtained for these quantities will change as a more detailed study is performed. For the structure, an assumed value was used for the non-load bearing components. However, since these components are not significantly related to the loading on the structure, any moderate change from the assumed value should not significantly impact the array structural results.

The power performance, however, can be significantly affected by a more detailed modeling of the PV blanket power profile. The analysis used to determine the power profile for the various PV blankets was based on the normal component of solar radiation falling on the projected blanket area. The analysis did not include reflected radiation and the thermal variation of the PV blanket. These two factors could substantially alter the calculated output of the array. One point should be mentioned. The thermal variation of the blanket would tend to reduce the PV cell efficiency, whereas the reflected sunlight from the surroundings would increase the array output. Therefore, these two factors would be working against each other, and their combined effect may not be that great. The interaction between the blanket cover glass and the solar radiation can also affect the power output. At high solar incidence angles most of the solar radiation is reflected. The amount of radiation reflected in this manner through a day cycle depends on both the cover glass properties and the blanket configuration.

There are other PV blanket characteristics, such as PV cell packing factor and blanket tensile strength, which can affect the structural design and array specifications. On most PV blankets the cell packing factor is fairly high, therefore, this should not substantially degrade the assumed blanket performance. The actual strength of the blanket can be a design consideration, since the cables are spaced every 0.5 m and the PV blanket would have to support its own weight between the cables. For the Mars based arrays, this issue is compounded by the force exerted on the PV blanket by the wind. For very fragile PV blankets such as amorphous silicon, it is very likely that some form of backing material would have to be used to help support the blanket. Another concern is that the curve of the blanket will produce a partial shading on the back side of the array. Consideration to the effect of shading on the blanket should be given since a partial illumination of a string of PV cells can short out the string. The blanket would have to be designed or orientated in such a way that the PV cell strings run parallel to the shading line.

Through the results of the analysis, various characteristics of the arrays became evident. It was determined that for both tent arrays the optimum end angle was 0°. That is the PV blanket should be allowed to hang as loose as possible while still maintaining the catenary shape. It should be noted that the analysis was performed only to the point of 0° end angle. Beyond this a portion of the PV blanket will be horizontal on the ground. This could be taken to its extreme by allowing the PV blanket to hang loose enough to form an upside down "T" shape. The results suggest that the specific power of the array continues to increase beyond the 0° end angle mark. Before conclusions like this are drawn certain points must be considered. The power profile of a PV blanket with this shape must be examined to determine how it varies throughout the day. Due to the change in structural loadings, a different structural design may be more appropriate from the one used in this study. The examination of an array with the

above mentioned shape is left for future study.

The dimension of the array which produced the optimum configuration was dependent on blanket end angle, array width tent angle and structural material. The other factor such as blanket type and (for Mars) wind velocity, only affected the array performance specifications but did not change the design point.

The array characteristics, such as small storage volume, passive deployment mechanism and high estimated performance, enable this design to be applicable to a wide variety of missions both on Earth and other planetary bodies.

APPENDIX A

The deployment mechanism of the array consists of a series of extendable and rotating columns, As they extend under the force of pressurized gas the PV blanket is deployed to its proper configuration. Once fully extended these columns lock into place allowing them to serve as structural members to support the array. The locking mechanism uses a spring loaded pin which extends through a hole at the end of the previously extended cylinder. A diagram showing the locking mechanism is given in figure A1.

The columns can be categorized into two types, initial and secondary. The initial deployment columns are used to orient the secondary columns, which in turn deploy the PV blanket. In order for the deployment to occur, the secondary columns must be capable of rotating into their proper orientation as they are being moved outward. This rotation is performed by brackets that connect the initial columns to the secondary columns. These brackets allow the secondary columns to have one rotational degree of freedom. The connection bracket also houses the pressure lines that allow the pressurized gas to pass between the columns. A diagram of the connection bracket and pressure lines is shown in figure A2.

The deployment sequence takes place in a series of steps as follows:

* The area where the array is to be located must be fairly level and cleared of obstacles which can inhibit deployment.

* Once the stowed array is placed in the cleared area, the top and sides of the array box, which are used to protect the array during transportation, are unfolded.

* The initial pressure valve, located on the pressure tank, is opened by remote control. It also has the ability to be remotely closed if a problem should arise during deployment and, if necessary, it can be operated manually.

* The pressurized gas enters the initial deployment cylinders causing them to extend.

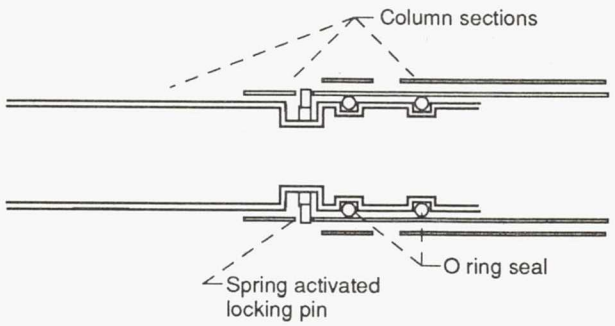

Figure A1.—Extendible column locking mechanism.

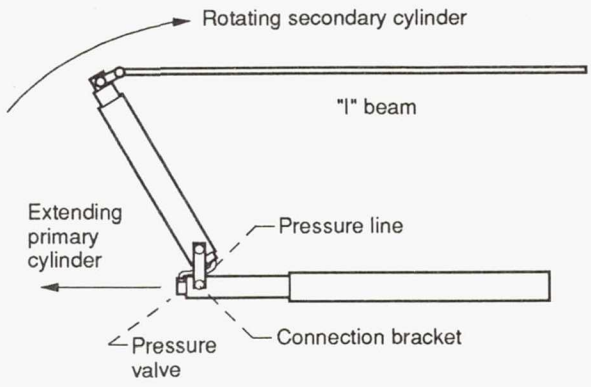

Figure A2.—Linkage between primary and secondary columns.

* As the initial columns extend the secondary columns are pushed and rotated into their deployment configuration. As the secondary columns are moved the PV blanket begins to unfold or unroll depending on the storage method. A small wheel, located at the end of each column in contact with the surface enables easier movement of the column over the surface.

* Once the initial deployment columns are extended, the array is in a semi-deployed configuration and the sequence is halted until the next series of valves are opened. These valves are located along the pressure lines connecting the initial columns to the secondary columns. The array is visually inspected to insure that no component is binding or in any other way inhibited from extending before the deployment is continued.

* Once full deployment is achieved the array is examined to insure the deployment was successful and that all cylinders are locked. As a safety precaution, the valves would then be moved to their vent position to depressurize the columns. A Guy wire connected to the vertical columns must then be secured to the ground to stabilize the structure. For Mars-based arrays, the structure itself must also be secured to the surface so that it is not moved or toppled by the wind.

* The array is now ready to be connected to the power management and distribution system.

If it is required, the array can be manually retracted into its stowed position. This is done by using a tool to push in the locking pins on the cylinders to allow them to collapse. As the array is being retracted the PV blanket will roll back onto the spring loaded storage roll or be folded back into its storage configuration. Once stowed the valves can be reset and the pressurized gas tank recharged so the array can be used again.

APPENDIX B

A	blanket area, m^2
A_{be}	beam cross sectional area, m^2
b	beam width, m
C_1	lift coefficient
c	catenary curve constant, m
E	Young's modulus of elasticity, Pa
F	applied force, N
h	beam height, m
I	moment of inertia, m^4
L	straight line length between PV blanket points 1 and 2, m
L_b	length of beam, m
L_{hc}	length of horizontal column, m
L_{vc}	length of vertical column, m
P	pressure, Pa
P_o	array output power, W
R_e	Reynolds number
r_i	inner radius, m
r_o	outer radius, m
SI	solar intensity, W/m^2
T_1	tension in cable at point 1, N
T_2	tension in cable at point 2, N
t	thickness, m
V_{tank}	pressurized gas tank volume, m^3
V_{total}	total system gas volume, m^3
v	velocity, m/s^2
w_b	distributed load on beam, N/m
w_c	distributed weight of PV blanket per cable, N/m
x	horizontal position along PV blanket, m
x_1	horizontal coordinate of point 1, m

x_2 horizontal coordinate of point 2, m

y_1 vertical coordinate of point 1, m

y_2 vertical coordinate of point 2, m

α angle of incident solar radiation

β solar evaluation angle

ε maximum beam bending, m

η_{sc} solar cell efficiency

θ angle of blanket normal to horizontal

θ_t tent angle

θ_1 blanket lower end angle

θ_2 blanket upper end angle

ρ density, kg/m^3

σ stress, Pa

τ atmospheric attenuation factor

Array Structural Analysis

The array structure is composed of beams, columns, cables, a pressurized gas tank and various other components such as pressure lines and movable brackets. Drawings showing the array and certain components are in figures 1, A1, and A2. The necessary size of each component was determined by calculating the moment of inertia required to withstand the various forces acting on that component. A factor of safety of 2 was incorporated into the component designs, except for the pressurized gas tank, where a factor of safety of 2.5 was used.

The main contribution to the stress in the structure is due to the tension in the cables which support the PV blanket. It was assumed that the cables would be incorporated within the array blanket and spaced every 0.5 m. Under the force of gravity a cable carrying a uniformly distributed load will take the shape of a catenary curve. The tension in the cables was determined by using equations to describe their shape under the given conditions. The conditions specified were lower end angle of the blanket with respect to the tent base and geometric proportions of the tend obtained from the desired tent angle. The proportions are determined by the selected tent angle, which is the angle from the base to a straight line between the blanket attachment points. This geometry is shown in figure B1 and the basic equations used to describe it are as follows:

$$y_1 = \frac{c}{\cos \theta_1} \tag{B1}$$

$$y_1 = c \cosh \frac{x_1}{c} \tag{B2}$$

$$y_2 = L \sin \theta_t + y_1 \tag{B3}$$

$$x_2 = L \cos \theta_t + x_1 \tag{B4}$$

$$y_2 = c \cosh \frac{x_2}{c} \tag{B5}$$

The above equations are combined in order to solve for c, while specifying only the lower end angle, θ_1, of the blanket and the straight line length, L, between the blanket attachment points. This yields:

$$L \sin \theta_1 + \frac{c}{\cos \theta_1} = c \times \left[\cosh\left(\frac{L}{c} \cos \theta_1\right) \frac{1}{\cos \theta_1} + \sinh\left(\frac{L}{c} \cos \theta_1\right) \sinh\left(\cosh^{-1} \frac{1}{\cos \theta_1}\right) \right] \tag{B6}$$

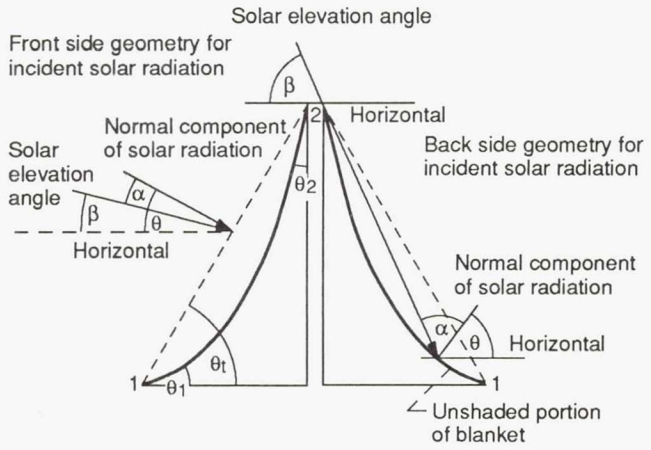

Figure B1.—Tent array PV blanket and solar radiation geometry.

Once the c value has been obtained the tension in the cable at the upper and lower attachment points to the structure can be calculated from the following:

$$T_1 = w_c y_1 \qquad \text{(B7)}$$

$$T_2 = w_c y_2 \qquad \text{(B8)}$$

where w_c is the distributed load on the cable due to the weight of the PV blanket.

The components of tension from each cable contribute to the horizontal and vertical forces seen by the upper and lower beams. Using the tension values as point loads along the beam, the required moment of inertia and hence size of the beam can be calculated. An I-beam shape was assumed, of which the expression for the moment of inertia is:

$$I = \frac{2bt^3 + th^3}{12} + bt(t + h)^2 \qquad \text{(B9)}$$

where b, t, and h are dimensions of the I-beam and are defined by figure B2.

Various combinations of b, t, and h can be used to obtain a given value of I. However to minimize mass one would like to choose the dimensions so that the minimum cross-sectional area is used while still maintaining the desired

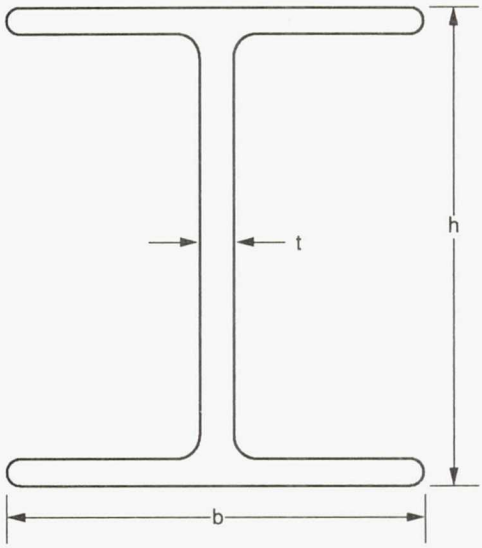

Figure B2.—I-beam dimensions.

moment of inertia value. For a h/t ratio of 16 the minimum area for a given I value is:

$$A_{be} = \frac{I}{289.16\, t^2} + 12.82\, t^2 \qquad \text{(B10)}$$

$$t = 0.128\, I^{0.25} \qquad \text{(B11)}$$

The required I value is obtained by selecting a maximum beam bending value and solving the following beam deflection equation.

$$I = \frac{5\left(\frac{L_b}{2}\right)^4 w_b}{384 F \varepsilon} \qquad \text{(B12)}$$

where the maximum allowed beam bending ε was set at 0.01 m. Solving this equation yields the required dimensions and therefore weight of the upper horizontal beam. This same process is performed on the lower two horizontal beams to obtain their dimensions and weight. The only difference is that for the beam at the top of the array the effective horizontal component of the tension is canceled since it is of equal strength and opposite direction on either side of the beam. For the lower beams the horizontal

component remains. To minimize mass on the lower beam it would have to be oriented so that the tension is applied axially through the center of the beam.

The columns are the next major structural component. They consist of a series of telescoping tubes which lock into place once fully extended. The columns are used as part of the base structure and as the main supports at the center of the array. These different positions produce different loadings and therefore different requirements for the columns. The vertical column will experience the greatest load in compression and therefore must be able to resist buckling. The horizontal column must be capable of withstanding a combination of compressive and bending loads. Moment of inertia values necessary to withstand the various loadings were calculated for both the horizontal and vertical columns. The column was then sized to accommodate the largest moment of inertia value necessary to withstand the forces exerted on it. The equations for the compressive and bending moment of inertia values are as follows:

$$\text{For compression} \quad I = \frac{FL_{vc}^2}{\pi^2 E} \tag{B13}$$

$$\text{For bending} \quad I = \frac{FL_{hc}^2}{3F\varepsilon} \tag{B14}$$

It should be noted that no bending loads were considered on the vertical columns. The reasoning behind this is that in order to support the columns from bending, Guy wires are attached to the top of the column and secured to the ground. The weight of using these wires is substantially less than that of sizing the columns to be structurally rigid enough to withstand the various bending moments they may be subjected to. After the necessary moment of inertia was determined, the column dimensions were calculated using the following equation:

$$I = \frac{\pi}{4}\left(r_o^4 - r_i^4\right) \tag{B15}$$

The column thickness was chosen to be 0.001 m.

Pressurized gas is used to extend the columns and deploy the array. The gas is stored in a tank which is connected to the columns by valves and pressure lines. As the array is deployed the total volume occupied by the gas increases and the pressure of the gas decreases. The initial gas pressure must be sufficient to overcome the greatest force on the columns while the gas occupies the total volume of the tank, lines and columns. Due to the necessary higher pressure seen by the columns during the beginning of deployment, they would tend to extend too quickly and may damage the array. This can be compensated for by increasing the damping on the initial column sections, thereby inducing slower movement. A possible way of accomplishing this is by increasing the frictional force between the cylinders by adding additional or thicker "O" rings. The tank size was set at 0.5 m long with a 0.1 m inner radius. The tank thickness was calculated so that it could accommodate the required pressure. The equation for tank thickness is as follows:

$$t = \frac{Pr_i}{\sigma} \tag{B16}$$

$$P = \frac{FV_{total}}{\pi r_i^2 V_{tank}} \tag{B17}$$

The last structural member is a beam used to support the pressurized gas tank and initial deployment columns. The dimensions and weight for this beam are calculated in the same manner as those for the beams used to support the PV blanket.

The tent structural analysis given previously was based on Lunar surface conditions. To adapt the array analysis to Mars the different environmental conditions must be incorporated into the calculations. This includes an increase in gravitational field strength and the addition of wind loadings due to the Martian atmosphere. The increase in gravitational field strength requires the various structural components to withstand greater moment of inertia values, thereby increasing their size and hence mass. The effect of wind loading on a structure can greatly affect its structural design characteristics. The average wind velocity on Mars is 6 to 8 m/s (ref. 5). The design wind velocity for the arrays was 20 m/s. This was chosen since 99.9 percent of the winds experienced on Mars are below 20 m/s (ref. 5). The wind will generate its largest force on the structure when it is oriented along the length of the array. In this situation the blanket would act as a sail. For an optimum wind angle of attack of 15°, and considering a low Reynolds number flow ($Re \leq 10^5$), the assumed maximum lift coefficient (C_l) is 1.5. The ideal conditions necessary to produce a lift coefficient for the blanket of 1.5 would be very rare. The equation which describes the force exerted on the structure by the wind is:

$$F = 0.5\ \rho\ v^2\ A\ C_l \qquad \text{(B18)}$$

The force is assumed to be exerted downward on the array, thereby increasing its effect by adding to the gravitational and tension forces.

A power profile for the array with each PV blanket type is necessary to enable an accurate comparison of performance between the arrays. The power profile is used to generate a figure of merit for the array in watts/kilogram. This figure of merit can then be used as a guideline for comparing the various arrays. The approximate power profiles which are used to determine the specific power of each array are based on the geometry of the array blanket and the incident solar radiation falling on the blanket. The power profiles are considered approximate, because factors such as reflected radiation and the blanket thermal profile have been neglected. A more detailed analysis taking into account these quantities must be performed if a true representation of the performance of a specific array is desired. Also, the analysis assumes that the array axis is perpendicular to the incident solar radiation. In other words the array would be located such that the sun passes directly overhead. By specifying a particular latitude and time of year, the power profile could change considerably.

For the purposes of this study, however, the approximate power profiles are sufficient to enable a good estimate for the performance of the array with the various PV blankets. By performing an in-depth power analysis the actual specific power may change from those obtained by the approximate analysis, but the trends and comparisons obtained from the approximation should be valid.

The power profile was generated by:

$$P_o = \eta_{sc} \tau\ A\ SI \cos \alpha \qquad \text{(B19)}$$

$$\alpha = |\theta - \beta| \qquad \text{(B20)}$$

A diagram showing the incident solar radiation angle and blanket geometry is shown in figure B1.

The above equation is used to calculate the power produced on one side of the tent. As the sun approaches the apex of the tent the backside will begin to be illuminated. Since the blanket is not pulled completely taut, some shading will occur on the backside of the array blanket until the solar elevation angle is 90°. The amount of shading will depend on the shape of the blanket. However since the power generation curve is based on the projected area of the blanket,

instead of the actual blanket area, the backside shading does not have an effect.

The value of τ for the Moon is 1 since there is no atmosphere and it is assumed to be 0.85 for Mars.

REFERENCES

1. Landis, G.A., et al.: Photovoltaic Power for a Lunar Base. Acta Astronaut., vol. 22, 1990, pp. 197-203.

2. Lovell, D.R.: Carbon Fiber Composite Reciprocating Guide Bar. Carbon Fibers, Technology, Uses and Prospects, The Plastics and Rubber Institute, London, England, 1986, pp. 176-182.

3. Piszczor, M.: Specifications of Various PV Blankets. Internal Report, Photovoltaics Branch, NASA Lewis Research Center, June 1990.

4. Hawak, J.J., et al.: Ultralight Amorphous Silicon Alloy Photovoltaic Modules for Space and Terrestrial Applications. Advancing Toward Technology Breakout in Energy Conversion (21st IECEC), Vol. 3, American Chemical Society, 1986, pp. 1436-1440.

5. West, G.S., Jr., et al., eds.: Space and Planetary Environmental Criteria Guidelines for Use in Space Vehicle Development. NASA TM-78119, 1977 Revision.

6. Gaier, J.R.; Perez-Davis, M.E.; and Marabito, M.: Aeolian Removal of Dust from Photovoltaic Surfaces on Mars. NASA TM-102507, 1990.

7. Appelbaum, J.; and Flood, D.J.: Photovoltaic Power System Operation in the Mars Environment. NASA TM-102075, 1989.

8. Allen, D.H.; and Haisler, W.E.: Introduction to Aerospace Structural Analysis. John Wiley and Sons, New York, 1985.

9. Appelbaum, J.; and Flood, D.J.: The Mars Climate for a Photovoltaic System Operation. NASA TM-101994, 1989.

10. Beer, F.P.; and Johnston, E.R., Jr.: Vector Mechanics for Engineers, Statics and Dynamics. 4th ed., McGraw-Hill, New York, 1984.

11. Beer, F.P.; and Johnston, E.R., Jr.: Mechanics of Materials. McGraw-Hill, New York, 1981.

12. Iles, P.A., et al.: Gallium Arsenide-on-Germanium Solar Cells. Proceedings of the 24th IECEC, Vol. 2, IEEE, 1989, pp. 791-797.

13. Rauscherback, H.S.: Solar Cell Array Design Handbook. Van Nostrand Reinhold, New York, 1980.

14. Winslow, C.; Bilger, K.; and Baraona, C.: Space Station Freedom Solar Array Design Development. Proceedings of the 24th IECEC, Vol.1, IEEE, 1989, pp. 283-287.

NASA
National Aeronautics and Space Administration

Report Documentation Page

1. Report No.	2. Government Accession No.	3. Recipient's Catalog No.
NASA CR-187119		

4. Title and Subtitle	5. Report Date
Design, Optimization, and Analysis of a Self-Deploying PV Test Array	6. Performing Organization Code

7. Author(s)	8. Performing Organization Report No.
Anthony J. Collozza	None (E-6252)
	10. Work Unit No. 593-14-11

9. Performing Organization Name and Address	11. Contract or Grant No.
Sverdrup Technology, Inc. Lewis Research Center Group 2001 Aerospace Parkway Brook Park, Ohio 44142	NAS3-25266
	13. Type of Report and Period Covered Contractor Report Final
12. Sponsoring Agency Name and Address National Aeronautics and Space Administration Lewis Research Center Cleveland, Ohio 44135-3191	14. Sponsoring Agency Code

15. Supplementary Notes

Project Manager, D.J. Bents, Power Technology Division, NASA Lewis Research Center. Portions of this material were presented at the 26th Intersociety Energy Conversion Engineering Conferences cosponsored by the ANS, SAE, ACS, AIAA, ASME, IEEE, and AIChE, Boston, Massachusetts, August 4-9, 1991. Responsible person, Anthony J. Colozza, (216) 433-5293.

16. Abstract

This study was performed in order to design a tent shaped PV array and optimize the design for maximum specific power. In order to minimize output power variation a tent angle of 60° was chosen. Based on the chosen tent angle an array structure was designed. The design considerations were minimal deployment time, high reliability and small stowage volume. To meet these considerations the array was chosen to be self-deployable, form a compact storage configuration, using a passive pressurized gas deployment mechanism. The array structural components consist of a combination of beams, columns and cables which are used to deploy and orient a flexible PV blanket to its proper configuration. Upon deployment pressurized gas is channeled to the columns causing them to extend, this deploys the PV blanket from the stowed configuration. Once extended the columns lock into place securing the structure. The arrangement and connection of the columns and the use of a thin flexible PV blanket was selected so that the array can be packaged into a relatively small volume. Each structural component of the design was analyzed to determine the size necessary to withstand the various forces it would be subjected to. Through this analysis the component weights were determined. An optimization was performed to determine the array dimensions and blanket geometry which produce the maximum specific power for a given PV blanket. This optimization was performed for both Lunar and Martian environmental conditions. Other factors such as PV blanket type, structural material and wind velocity (for Mars array), were varied to determine what influence they had on the design point. The analysis showed that the variation of these parameters did not significantly affect the design points. These factors did, however, influence the array performance values, such as specific power and specific mass, at the design point. The performance specifications for the array at both locations and with each type of PV blanket were determined. These specifications were calculated using Arimid fiber composite as the structural material. This material produced the lowest specific mass out of the ones which were examined. The four PV blanket types considered were Silicon, GaAs/Ge, GaAs CLEFT and Amorphous Silicon. The specifications used for each blanket represented either present day or near term technology. For both the Moon and Mars the Amorphous Silicon arrays produced the highest specific power.

17. Key Words (Suggested by Author(s))	18. Distribution Statement
Photovolatic conversion; Solar power generation; Solar arrays; Space erectable structures; Structural design; Telescoping structures	Unclassified - Unlimited Subject Category 44

19. Security Classif. (of the report)	20. Security Classif. (of this page)	21. No. of pages	22. Price*
Unclassified	Unclassified	18	A03

NASA FORM 1626 OCT 86

*For sale by the National Technical Information Service, Springfield, Virginia 22161